

## Supramolecular Catalysis of the Enantiodifferentiating [4 + 4] Photocyclodimerization of 2-Anthracenecarboxylate by $\gamma$ -Cyclodextrin

Asao Nakamura\*<sup>†</sup> and Yoshihisa Inoue\*<sup>‡</sup>

Contribution from the Inoue Photochirogenesis Project (ERATO) and Entropy Control Project (ICORP), JST, 4-6-3 Kamishinden, Toyonaka 560-0085, Japan

Received May 22, 2001; E-mail: asao@chiromor.jst.go.jp; inoue@chem.eng.osaka-u.ac.jp

**Abstract:** 2-Anthracenecarboxylic acid (AC) makes a very stable 1:2 inclusion complex with  $\gamma$ -cyclodextrin ( $\gamma$ -CDx) ( $K_1 = 161 \pm 25 \text{ M}^{-1}$ ,  $K_2 = 38\,500 \pm 3300 \text{ M}^{-1}$  at 25 °C). The formation of the 1:2 inclusion complex accelerated the photocyclodimerization of AC. The 1:2 inclusion could be clearly verified by UV-vis, CD, and  $^1\text{H}$  NMR spectroscopies. Although these spectroscopies provide little information about the structural isomers of the inclusion complex, there should be several structural isomers of the 1:2 inclusion complex which have a different longitudinal orientation of the guest molecules in the cavity. The isomer distribution of the photodimerization product primarily depends on the population of these orientational isomers of the 1:2 inclusion complex in the ground state before photoreaction, because, in the lifetime of the excited singlet state, exchanging the orientation is impossible. The enantioselectivity of the photodimerization originates from the difference in the stability of the diastereomeric pair of orientational isomers of the 1:2 inclusion complex in the ground state, which are the precursors of the enantiomers of a specific chiral cyclodimer. The ee of a chiral cyclodimer **2** was 32% at 25 °C and was enhanced by lowering the temperature to 41% at 0 °C. This is the highest value reported for the asymmetric photodimerization in solution.

### Introduction

In organic photochemistry, the chirality control of reactions has been a major topic over the past few decades.<sup>1-3</sup> The asymmetric photochemical reactions are classified into two categories. The first one includes the reactions in which the chirality is transferred within a molecule from the chiral auxiliary to the reacting moiety. So far, this approach has been the most successful in asymmetric photochemistry.<sup>4</sup> By this approach, high diastereomeric excesses can be induced through the intramolecular interaction between the chiral auxiliary and the reacting moiety. The second category includes the reactions in which the chirality is transferred from one molecule to the other molecule. In this category, the reactions reported by Inoue

et al. are the most successful examples.<sup>5</sup> They have reported that the *E-Z* photoisomerization of cyclooctene enantioselectively takes place in high enantiomeric excesses (ee's) when the reaction is sensitized by chiral alkyl benzoates.

The chirality induction during the photocycloaddition of achiral (prochiral) substrates is possible only through the intermolecular interaction between the substrate in the excited state and the chiral group of a neighboring molecule. The chiral group, which plays a crucial role in the enantiodifferentiation, may be attached to a chiral sensitizer, which transfers the excitation energy to the substrate (chiral photosensitizer method), or be a part of the molecules surrounding the substrate in the excited state (chiral template method). Kim and Shuster reported that the [4 + 2] photocycloaddition of trans- $\beta$ -methylstyrene with cyclohexa-1,3-diene sensitized by (-)-1,1'-bis(2,4-dicyanonaphthalene) produced a nonracemic cyclodimer.<sup>6</sup> Recently, Inoue et al. have also reported that, by using chiral naphthalenecarboxylates as photosensitizers, the cycloaddition of alcohols to 1,1-diphenylalkenes enantioselectively proceeds.<sup>7</sup> However, for the latter approach, only a few examples have been reported.

Bach et al. recently reported the enantioselective intermolecular [2 + 2] photocycloaddition of alkenes and a 2-quinolone in solutions using a chiral lactam host.<sup>8</sup> They succeeded in protecting one of the prochiral faces of the substrate 2-quinolone

<sup>†</sup> Present address: Kuroda Chiromorphology Project, ERATO, JST, 4-7-6 Komaba, Meguro-ku, Tokyo 153-0041, Japan. Tel. & Fax: +81-3-5465-0104.

<sup>‡</sup> Permanent address: Department of Molecular Chemistry, Faculty of Engineering, Osaka University, 2-1 Yamada-oka, Suita 565-0871, Japan. Tel.: +81-6-6879-7920. Fax: +81-6-6879-7923.

- (1) For historical background, see: (a) Kagan, H. B.; Fiand, J. C. *Top. Stereochem.* **1978**, 10. (b) Rau, H. *Chem. Rev.* **1983**, 83, 535. (c) Inoue, Y. *Chem. Rev.* **1992**, 92, 741.
- (2) For a more recent review, see: Everitt, S. R. L.; Inoue, Y. In *Organic Photochemistry; Molecular and Supramolecular Photochemistry*; Ramamurthy, V., Schanze, K. S., Eds.; Marcel Dekker: New York, 1999; Vol. 3, p 71.
- (3) For the reviews on the asymmetric photochemistry in crystals: (a) Feringa, B. L.; van Delden, R. A. *Angew. Chem., Int. Ed.* **1999**, 38, 3418. (b) Ito, Y. In *Organic Photochemistry; Molecular and Supramolecular Photochemistry*; Ramamurthy, V., Schanze, K. S., Eds.; Marcel Dekker: New York, 1999; Vol. 3, p 1.
- (4) Pete, J.-P. In *Adv. Photochem.*; Neckers, D. C., Volman, D. H., von Bünau, G., Eds.; John Wiley & Sons: New York, 1996; Vol. 21, p 135.

(5) Inoue, Y.; Wada, T.; Asaoka, S.; Sato, H.; Pete, J.-P. *J. Chem. Soc., Chem. Commun.* **2000**, 251.

(6) Kim, J.-I.; Schuster, G. B. *J. Am. Chem. Soc.* **1990**, 112, 9635.

(7) Asaoka, S.; Ooi, M.; Jiang, P.; Wada, T.; Inoue, Y. *J. Chem. Soc., Perkin Trans. 2* **2000**, 77.

from attack by alkenes. Complementary hydrogen bonding was used for the binding of the 2-quinolone to the lactam host. However, the application of such an approach might be rather limited, because designing a fit host for a specific substrate is not always easy.

There is another category of chiral hosts which accepts a variety of guests with a low specificity. Cyclodextrins are typical hosts belonging to this category. They may be useful for controlling the enantioselectivity of the photocycloaddition.<sup>9</sup> Among the other cyclodextrins,  $\gamma$ -cyclodextrin ( $\gamma$ -CDx) is particularly attractive, because it is able to accommodate two molecules of aromatic compounds into its chiral cavity. The co-inclusion of two molecules within a cavity is expected to accelerate the cycloaddition. Actually, the acceleration and the switching in the regioselectivity of the photocyclodimerization have been reported for anthracene derivatives,<sup>10,11</sup> coumarin derivatives,<sup>12,13</sup> tranilast,<sup>14</sup> stilbene derivatives,<sup>15,16</sup> and stilbazole.<sup>17</sup> At the same time, the chirality of the CDx cavity interior is expected to provide the potential energy gradient, promoting the enantiodifferentiating approach of the substrates.

Tamaki et al. reported that the prochiral anthracenecarboxylic acids were very efficiently cyclodimerized to form cyclodimers including chiral ones.<sup>10</sup> The enantiodifferentiation during the photocyclodimerization was proven by the circular dichroism (CD) spectrum of the isolated fraction from achiral HPLC containing both enantiomers of one of the chiral cyclodimers. However, they have never assessed the magnitude of the ee. Ueno et al. examined the possibility of chiral induction by the chiral CDx cavity using a different approach.<sup>18</sup> They synthesized a bis-anthracenecarboxylate-modified  $\gamma$ -CDx. Photoirradiation of the compound yielded the intramolecular cyclodimer of the anthracene moieties, which was hydrolyzed to give the cyclodimer of anthracenecarboxylic acid. The hydrolysis product exhibited optical activity in the CD spectrum. This also implies that the chirality of the CDx cavity is effective for inducing enantioselectivity in the photocyclodimerization. Unfortunately, however, they did not estimate the ee of the hydrolysis products.

Recently, we have succeeded in the chromatographic resolution of the enantiomers and the estimation of ee of chiral photocyclodimers of 2-anthracenecarboxylic acid (AC). In the present study, we quantitatively examined the ability of the CDx cavity to induce chirality during the photocyclodimerization of AC and further revealed the mechanisms and factors controlling the product ratio and ee.

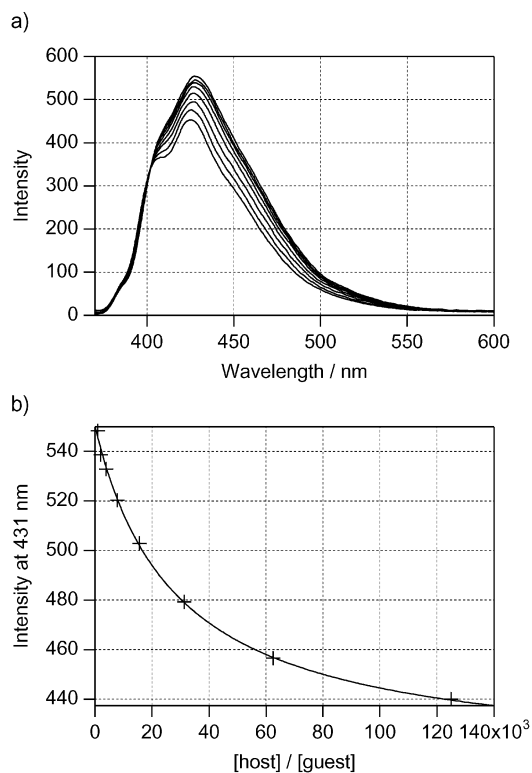


**Figure 1.** (a) Fluorescence spectra of a 0.2  $\mu$ M solution of AC at various concentrations of  $\gamma$ -CDx. (b) Plot of the fluorescence intensity at 431 nm versus the  $\gamma$ -CDx concentration. The curve in the figure is the best fit curve obtained by a nonlinear least-squares fitting procedure assuming the 1:1 complexation of  $\gamma$ -CDx with AC. The obtained association constant was  $167 \pm 25 \text{ M}^{-1}$ .

## Results

### Stoichiometry and Stability of the Inclusion Complexes

**of  $\gamma$ -CDx with AC.** The stoichiometry of the complexation of  $\gamma$ -CDx with 2-anthracenesulfonate (AS) has been reported by Tamaki et al. They established the scheme for the formation of a 1:2 host:guest inclusion complex, assuming stepwise formation through 1:1 complexation. We could use AS instead of AC in the following study of the enantiodifferentiating photocyclodimerization. However, the photocyclodimers of AS exhibited a poorer resolution on chiral HPLC columns than AC. Therefore, we used AC rather than AS. The scheme for the complexation of AC with  $\gamma$ -CDx was described by Tamaki et al. to be the same as that for AS. However, the scheme has never been verified. Therefore, we first examined the stoichiometry and stability of the inclusion complexes of AC with  $\gamma$ -CDx.

The addition of  $\gamma$ -CDx to a very dilute solution (0.2  $\mu$ M) of AC resulted in a decrease in fluorescence intensity (Figure 1). A plot of the fluorescence intensity versus the concentration of  $\gamma$ -CDx fit very well to the curve calculated assuming a 1:1 complex formation, giving a stability constant ( $K_1$ ) of  $161 \pm 25 \text{ M}^{-1}$ . The 1:1 inclusion complex exhibited a fluorescence with a lifetime of 10 ns, which was shorter than that of the free AC (16 ns).

At a much higher AC concentration, a new complex with a different stoichiometry formed. A Job plot of the change in the UV-vis absorption spectrum gave a peak at the ratio of  $[\gamma\text{-CDx}]:[\text{AC}] = 1:2$ , when  $[\gamma\text{-CDx}] + [\text{AC}] = 1 \text{ mM}$  (Figure 2). This means that the major species in this concentration region is a 1:2 complex. Another Job plot using the CD intensity at

- (8) (a) Bach, T.; Bergmann, H. *J. Am. Chem. Soc.* **2000**, *122*, 11525. (b) Bach, T.; Bergmann, H.; Grosch, B.; Harms, K. *J. Am. Chem. Soc.* **2002**, *124*, 7982.
- (9) Pushkara Rao, V.; Turro, N. J. *Tetrahedron Lett.* **1989**, *30*, 4641.
- (10) (a) Tamaki, T. *Chem. Lett.* **1984**, 53. (b) Tamaki, T.; Kokubu, T. *J. Inclusion Phenom.* **1984**, *2*, 815. (c) Tamaki, T.; Kokubu, T.; Ichimura, K. *Tetrahedron* **1987**, *43*, 1485.
- (11) Tamagaki, S.; Fukuda, K.; Maeda, H.; Mimura, N.; Tagaki, W. *J. Chem. Soc., Perkin Trans. 2* **1995**, 389.
- (12) Moorthy, J. N.; Venkatesan, K.; Weiss, R. G. *J. Org. Chem.* **1992**, *57*, 3292.
- (13) (a) Brett, T. J.; Alexander, J. M.; Stezowski, J. J. *J. Chem. Soc., Perkin Trans. 2* **2000**, 1095. (b) Brett, T. J.; Alexander, J. M.; Stezowski, J. J. *J. Chem. Soc., Perkin Trans. 2* **2000**, 1105.
- (14) Utsuki, T.; Hirayama, F.; Uekema, K. *J. Chem. Soc., Perkin Trans. 2* **1993**, 109.
- (15) Herrmann, W.; Wehrle, S.; Wenz, G. *J. Chem. Soc., Chem. Commun.* **1997**, 1709.
- (16) Rao, K. S. S. P.; Hubig, S. M.; Moorthy, J. N.; Kochi, J. K. *J. Org. Chem.* **1999**, *64*, 8098.
- (17) Banu, H. S.; Lalitha, A.; Pitchumani, K.; Srinivasan, C. *J. Chem. Soc., Chem. Commun.* **1999**, 607.
- (18) Ueno, A.; Moriwaki, F.; Iwama, Y.; Suzuki, I.; Osa, T.; Ohta, T.; Nozoe, S. *J. Am. Chem. Soc.* **1991**, *113*, 7034.

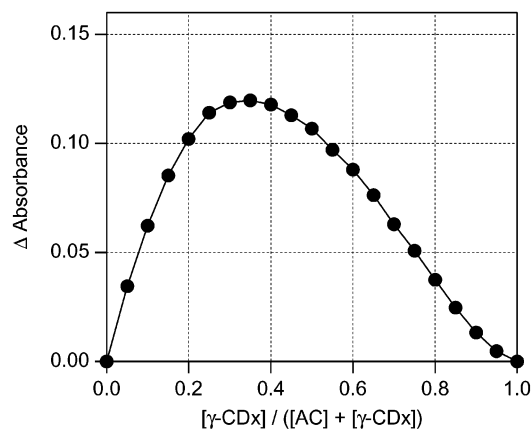


**Figure 2.** Job plot of the change in the UV-vis absorption spectrum showing the stoichiometry of the complexation of  $\gamma$ -CDx with AC. The  $\Delta$  absorbance at 335 nm was used for the plot.  $[\gamma\text{-CDx}] + [\text{AC}] = 1 \text{ mM}$ .

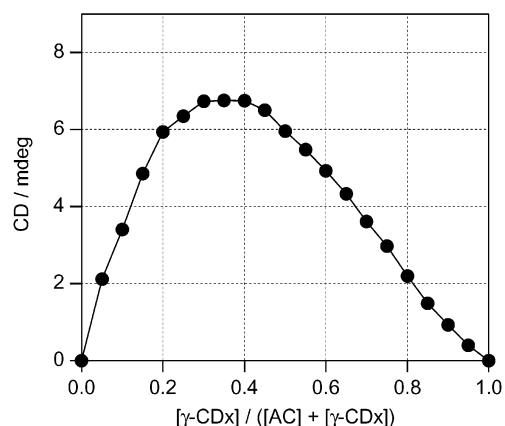
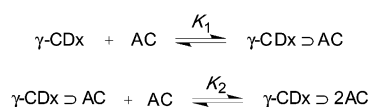


**Figure 3.** Job plot of the change in the CD spectrum showing the stoichiometry of the complexation of  $\gamma$ -CDx with AC. The CD intensities at 335 and 397 nm were used for the plot.  $[\gamma\text{-CDx}] + [\text{AC}] = 1 \text{ mM}$ .

#### Scheme 1



335 or 397 nm supported the same stoichiometry (Figure 3). Moreover, a plot of the absorbance at 387 nm versus the  $\gamma$ -CDx concentration for the titration of a 0.6 mM AC solution with  $\gamma$ -CDx fit well to the curve calculated assuming stepwise 1:1 and 1:2 complexations (Scheme 1; Figure 4). The stability constant for the association of AC with the already formed 1:1 complex ( $K_2$ ) of  $38\,500 \pm 3300 \text{ M}^{-1}$  was obtained.

**Temperature Dependence of the Stability Constants for the Inclusion Complexes of  $\gamma$ -CDx with AC.** The  $K_1$  and  $K_2$  values were measured at various temperatures between 5 and 60 °C (Table 1). The van't Hoff plots of the stability constants gave a straight line within the errors of the estimated values of the  $K$ 's (Figure 5). From the slopes and the intercepts, the  $\Delta H$  and  $T\Delta S$  for the formation of the complexes were obtained. For the 1:1 complex,  $\Delta H = -9.2 \pm 1.0 \text{ kJ mol}^{-1}$ , and  $T\Delta S = 3.4 \pm 1.0 \text{ kJ mol}^{-1}$ . For the 1:2 complex,  $\Delta H = -47.9 \pm 1.4 \text{ kJ mol}^{-1}$ , and  $T\Delta S = -21.2 \pm 1.4 \text{ kJ mol}^{-1}$ .

A primitive molecular modeling showed that a large space remains in the cavity of the 1:1 inclusion complex. This results in a relatively weak van der Waals (vdW) interaction, that is, a small negative  $\Delta H$  value. However, in the 1:2 complex, the

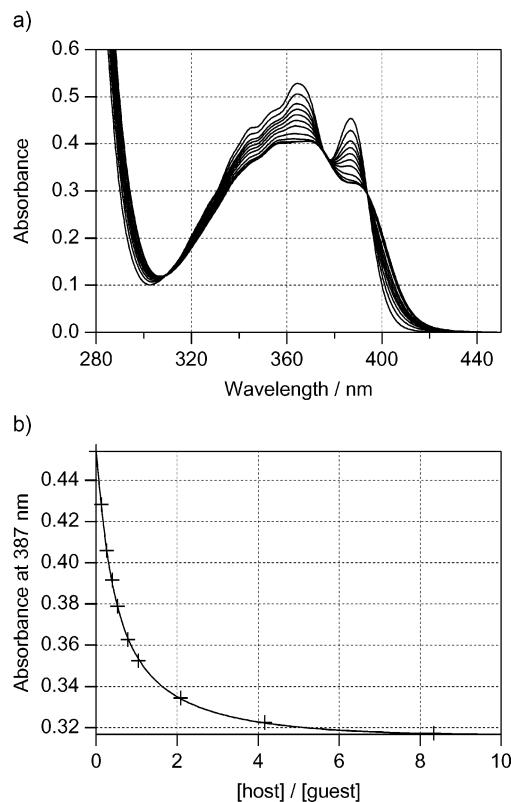


**Figure 4.** (a) UV-vis absorption spectra of a 0.6 mM solution of AC at various concentrations of  $\gamma$ -CDx. (b) Plot of the absorbance at 387 nm versus  $\gamma$ -CDx concentration. The curve in the figure is the best fit curve obtained by a nonlinear least-squares fitting assuming stepwise 1:2 complexation between AC and  $\gamma$ -CDx. In the fitting process, the association constant for the 1:1 complex was fixed at  $167 \text{ M}^{-1}$ . The obtained association constant for the second guest was  $38\,500 \pm 3300 \text{ M}^{-1}$ .

**Table 1.** Association Constants for the 1:1 and 1:2 Inclusion Complexes of  $\gamma$ -CDx with AC Obtained by Fluorescence and UV-Absorption Titrations at Various Temperatures

temperature /°C	association constant <sup>a</sup> /M <sup>-1</sup>			
	$K_1^b$	(16)	$K_2^c$	(30 000)
5	206	(16)	201 000	(30 000)
10	185	(31)	121 000	(11 000)
20	182	(22)	56 700	(10 800)
25	161	(25)	38 500	(3300)
30	156	(20)	31 100	(3100)
40	144	(14)	20 400	(2300)
50	124	(10)	10 400	(1700)
60	100	(10)	5710	(580)

<sup>a</sup> The values in parentheses are the errors. <sup>b</sup> Association constant for  $\gamma$ -CDx and AC making 1:1 complex. <sup>c</sup> Association constant for the 1:1 complex and AC making 1:2 complex.

area of the vdW contact between the host and the guest becomes significantly larger, resulting in a large negative  $\Delta H$  value. The large difference in the value of  $\Delta H$  between the 1:1 and 1:2 complexes enhances the preference of the 1:2 complex, especially at low temperature.

**Structure of the 1:2 Complex Analyzed by NMR Spectra.** The <sup>1</sup>H NMR spectra were measured for analyzing the 3-D structure of the inclusion complex. All of the signal peaks for the aromatic protons of AC are shifted upfield upon the complexation with  $\gamma$ -CDx (Figure 6). This is the result of the ring current of the nearby AC molecule and is the clear evidence for the co-inclusion of two AC molecules into the same cavity.

In the ROESY spectra, in the region showing the correlation between the peaks for the CDx protons and those for the AC

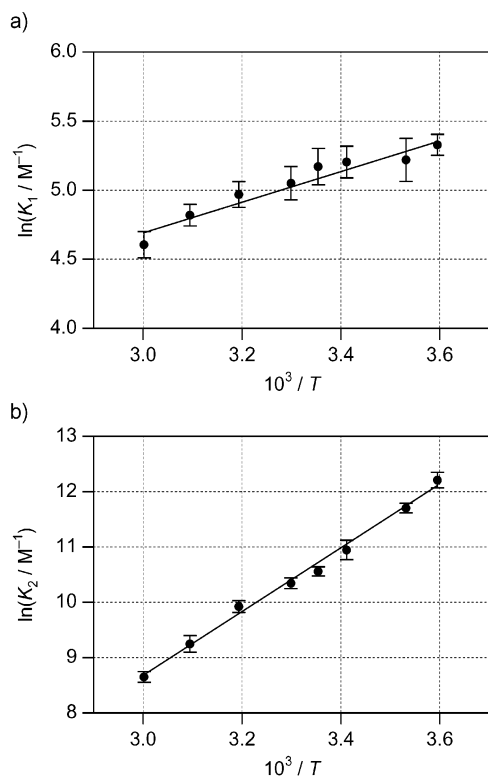


Figure 5. van't Hoff plots of the stability constants  $K_1$  (a) and  $K_2$  (b).

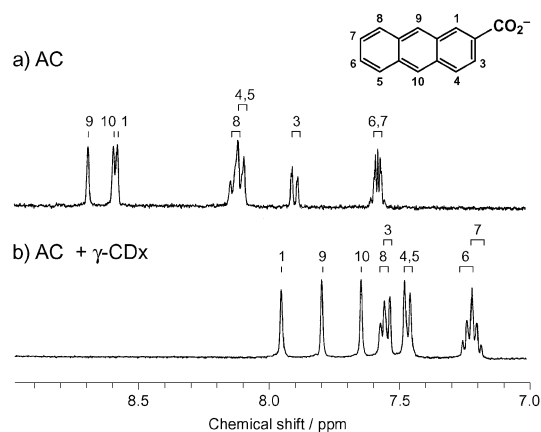


Figure 6. Aromatic region of the  $^1\text{H}$  NMR spectra of the  $\text{D}_2\text{O}$  solutions of (a) 2 mM AC and (b) 4 mM AC + 4 mM  $\gamma$ -CDx, at pH 9 and 30 °C.

protons, we could observe the cross-peaks correlating H-3 of CDx to H-1, H-4, H-5, H-8, H-9, and H-10 of AC, and H-5 of CDx to H-9, H-10, and H-1 of AC (Figure 7). If we assume that the observed signal is the average of the signals for several orientational isomers of the inclusion complex, these correlations can be rationalized by the molecular modeling. There can be two orientations for each AC molecule in a cavity, that is, orientations with the carboxylate group to the wider end and to the narrower end (Figure 8). The H-9 and H-10 of AC are always close to the H-5 of CDx in both orientations, which give strong cross-peaks. The H-1, H-4, H-5, and H-8 of AC are close to the H-3 of CDx in only one of the orientations, which give weaker cross-peaks.

These results imply that the structure of each isomer of the inclusion complex is well-defined, but there are several orientational isomers due to the longitudinal orientation of the AC molecule within the cavity.

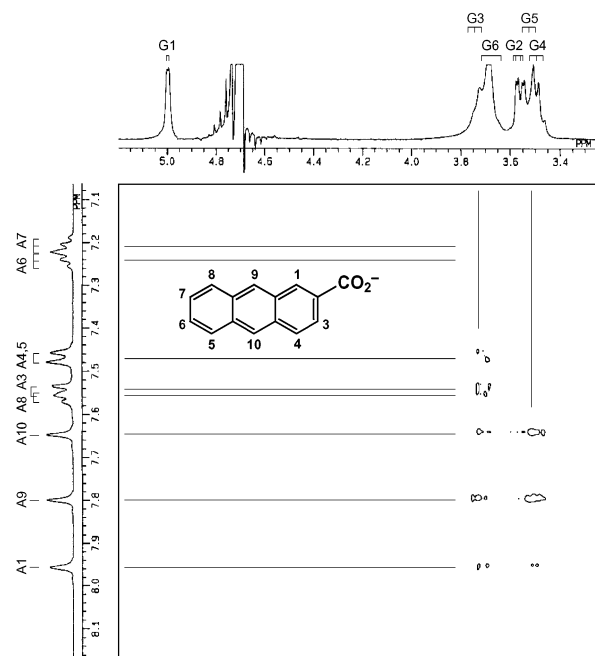


Figure 7. Portion of 2-D ROESY spectrum of the solution containing 4 mM AC and 4 mM  $\gamma$ -CDx at pH 9 and 30 °C.

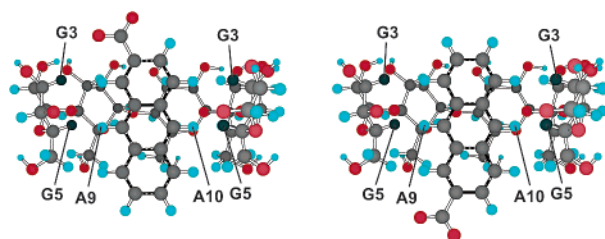


Figure 8. Plausible structure of the inclusion complex of  $\gamma$ -CDx with AC.

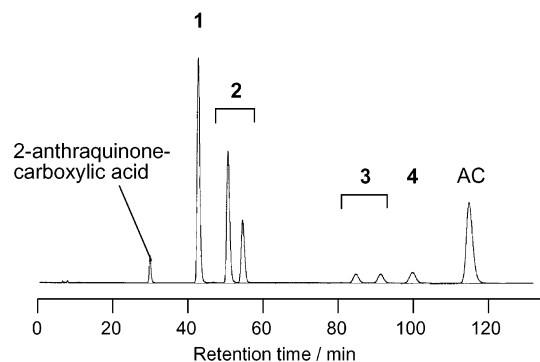
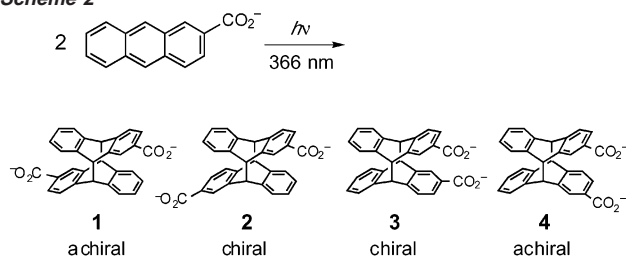


Figure 9. Typical HPLC chromatogram of the photoirradiated solution of AC.

**Chromatographic Resolution of the Isomers of the Cyclodimer of AC.** An aqueous solution of AC at pH 9 was irradiated in an Ar atmosphere at 366 nm using a medium-pressure mercury lamp. The reaction mixture was analyzed by HPLC using an achiral reverse-phase column (Figure 9). The chromatogram exhibited five product peaks, which were assigned to 2-anthraquinonecarboxylic acid and four regioisomers of the cyclodimer of AC (Scheme 2).<sup>10</sup> Two of the four could be resolved into enantiomers by the HPLC using chiral columns. By using the tandem columns of the achiral and one of the chiral columns, we directly resolved the product into the six stereoisomers and the quinone at once. This was very useful for

Scheme 2

**Table 2.** Photodimerization of AC in Aqueous Buffer Solutions at pH 9 in the Presence of  $\gamma$ -CDx<sup>a</sup>

run #	[AC] /mM	[ $\gamma$ -CDx] /mM	host/guest ratio	relative yield (%) <sup>b</sup>				% ee <sup>bc</sup>	
				1	2	3	4	2	3
1	0.4	0	0.0	42.0	36.0	13.8	8.1	-0.6	-0.9
2	0.4	0.1	0.25	42.8	43.2	8.4	5.6	28.2	-0.9
3	0.4	0.2	0.5	43.0	43.8	7.8	5.4	30.9	-2.4
4	0.4	0.4	1	43.0	44.0	7.6	5.4	31.6	-2.7
5	0.4	2	5	43.0	44.4	7.4	5.2	32.4	-2.4
6	0.4	4	10	42.9	44.7	7.3	5.2	32.0	-3.5
7	0.1	4	40	43.1	44.6	7.2	5.1	31.8	-4.7
8	0.8	4	5	43.0	44.6	7.2	5.2	31.8	-3.1
9	4	4	1	43.0	44.3	7.4	5.3	31.8	-2.8

<sup>a</sup> Solutions were made with 25 mM borate buffer (pH 9) and photoirradiated in an Ar atmosphere at 366 nm using a medium-pressure mercury lamp equipped with optical glass filters (Toshiba UV-35 and UV-D36C). <sup>b</sup> Relative yield and % ee were determined by the peak area on the HPLC chromatogram detected by the absorbance at 254 nm. The product distribution and % ee were nearly independent of the conversion. <sup>c</sup> Absolute configuration has never been determined. The sign of the ee is defined so that it is positive, if the yield of the first enantiomer on the chromatogram is higher than the second one. Errors in the values of % ee are  $\pm 0.5\%$  for isomer 2 and  $\pm 3\%$  for isomer 3.

**Table 3.** Effect of Temperature on the Product Distribution and % ee of the Photodimers of AC<sup>a</sup>

temperature /°C	relative yield (%)				% ee	
	1	2	3	4	2	3
0	42.9	46.3	6.1	4.7	41.2	-1.2
10	42.7	45.6	6.7	5.0	37.7	-1.8
20	43.0	44.8	7.0	5.2	33.9	-1.4
25	42.9	44.7	7.3	5.2	32.0	-2.5
30	43.3	43.6	7.7	5.4	30.4	-1.1
40	43.4	43.1	8.1	5.5	27.1	-2.8
50	43.7	42.0	8.6	5.8	23.8	-5.1
60	43.7	41.2	9.2	5.8	20.7	-4.3

<sup>a</sup> [AC] = 0.4 mM; [ $\gamma$ -CDx] = 4 mM. For reaction conditions in detail, see Table 2.

observing the product isomer distribution and estimating the enantiomeric excess (ee) of the chiral product isomers.

**Enantiodifferentiating Photocyclodimerization of AC in the Presence of  $\gamma$ -CDx.** As shown in Table 2, the photoirradiation of the solution of AC in the absence of  $\gamma$ -CDx provided all six isomers with a preference for the achiral isomer 1. In the presence of  $\gamma$ -CDx, the isomer distribution was slightly biased to give a higher yield of isomer 2 at the expense of isomers 3 and 4. The isomer distribution was virtually independent of the concentration of AC or  $\gamma$ -CDx under the conditions employed.

The addition of the  $\gamma$ -CDx induced the enantiodifferentiating photocyclodimerization of AC. The ee of the product isomer 2 was 32% at high host/guest ratios. The ee of the other chiral product isomer 3 was about 3% (the minus sign for the values in the table means that the preferred enantiomer eluted later than the antipode from the HPLC columns). The ee was nearly independent of the concentration of AC or  $\gamma$ -CDx under the

**Table 4.** Estimated Populations of the Free and Complex Species in the Solution Used for the Photoreaction

run # <sup>a</sup>	[AC] /mM	[ $\gamma$ -CDx] /mM	host/guest ratio	population <sup>b</sup> (%)			contribution of 1:2 species <sup>c</sup> (%)
				free AC	1:1	1:2	
1	0.4	0	0.0	100	0	0	0.0
2	0.4	0.1	0.25	80.3	0.8	18.9	65.1
3	0.4	0.2	0.5	68.0	1.5	30.5	77.8
4	0.4	0.4	1	53.9	2.6	43.5	86.0
5	0.4	2	5	26.8	7.9	65.3	93.8
6	0.4	4	10	19.1	11.7	69.2	94.7
7	0.1	4	40	31.5	20.0	48.5	88.3
8	0.8	4	5	14.6	8.5	76.9	96.4
9	4	4	1	9.1	3.1	87.8	98.3

<sup>a</sup> Run numbers correspond to those in Table 2. <sup>b</sup> Populations were estimated on the basis of the association constants obtained by titration experiments (Table 1). <sup>c</sup> Weight of the contribution of the 1:2 species to the formation of cyclodimers among those of the free AC, 1:1, and 1:2 species. These values were calculated by assuming that the quantum yield of the cyclodimers is 0.4 for the 1:2 species and 0.05 for the free AC.

conditions employed, except that, at a low host/guest ratio, a slight decrease in the ee was observed.

**Temperature Dependence of the Product Distribution and % ee of the Cyclodimer of AC.** Reaction temperature affects the ee's of photoproducts 2 and 3 (Table 3). By lowering the temperature, we enhanced the ee of isomer 2 from 21% ee at 60 °C to 41% ee at 0 °C, while the ee of 3 was decreased from -5% to -1% in the same temperature range. In addition to the higher ee's obtained for 2, lowering the temperature also appreciably enhanced the production of isomer 2 at the expense of the other isomers, in particular, 3 and 4.

## Discussion

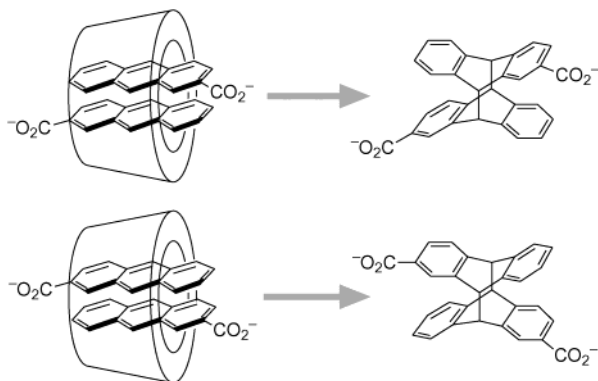
From the association constants obtained, we can calculate the distribution of each AC species in the solutions. Among the other complexes, the 1:2 species accounts for 18.9–87.8% of the total AC molecules in the solutions (Table 4). If the host/guest ratio is 0.5, the 2:2 species covers only 18.9% of the total AC species. Although 18.9% is not the majority, it is reasonable to consider that the major source of the cyclodimer is the 1:2 species, because the quantum yield of the photodimerization from the 1:2 complex is reported to be 8 times greater than that from free monomer. The photodimerization from the 1:1 complex should be much slower than that of the free monomer. Therefore, the contribution of the sum of the free monomer and 1:1 complex to the cyclodimer formation should be less than 35%, even though the population of these species is 81.1%. At the host/guest ratio of 1, the contribution of these species is less than 14%. Therefore, the isomer distribution and the ee's of the chiral products were virtually independent of the concentration of AC or  $\gamma$ -CDx under the conditions employed.

The coexistence of the free molecule of AC and 1:1 species with the 1:2 species might not be negligible especially at higher temperature. To check this, the population of each species at each temperature was estimated by using the equilibrium coefficients obtained at the same temperature (Table 5). The population of the 1:2 species was as high as 38% even at 60 °C. On the basis of the discussion in the previous section, this population is sufficient for proving that the major source of the cyclodimers is the 1:2 complex. The contribution of the 1:2 species to the formation of the cyclodimers is at least 83.1% at this temperature. Therefore, the lower ee of 2 at higher temperature is not the result of the destruction of the inclusion complex by lowering the stability.

**Table 5.** Estimated Populations of the Free and Complex Species in the Solution Used for the Photoreaction at Various Temperatures

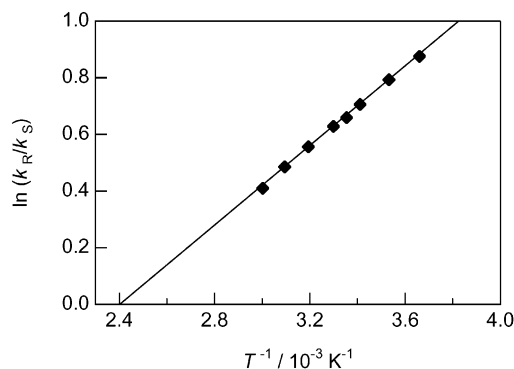
temperature /°C	population <sup>a</sup> (%)			contribution of 1:2 species <sup>a</sup> (%)
	free AC	1:1	1:2	
5	6.9	5.9	87.2	98.2
10	10.4	7.8	81.8	97.3
20	15.1	9.9	75.0	96.0
25	19.1	11.7	69.2	94.7
30	20.9	12.1	67.0	94.2
40	27.9	14.4	57.7	91.6
50	35.6	16.5	47.9	88.0
60	43.6	18.3	38.1	83.1

<sup>a</sup> [AC] = 0.4 mM; [ $\gamma$ -CDx] = 4 mM. See also footnote of Table 4.

**Figure 10.** Correlation between the diastereomeric 1:2 complexes before reaction and the enantiomers of one of the product isomers **2**.

There should be several structural isomers of the 1:2 inclusion complex which have a different longitudinal orientation of the guest molecules in the cavity. The product isomer distribution primarily depends on the population of these orientational isomers in the ground state before photoreaction. The transformation among these isomers takes place through two processes: the breaking of the inclusion complex into the 1:1 complex and free AC, and the reassociation of them into the 1:2 complex with a different orientation. This is because there is not enough space for the guest molecule to change its orientation within the cavity. Especially, in the lifetime of the excited singlet state, exchanging the orientation by these processes is impossible. In this situation, the enantiomers of **2** should be obtained from the relevant diastereomeric precursor complexes which are shown in Figure 10. The ee of **2** depends on the population of these diastereomeric precursor complexes in the ground state. The ee may also be affected by the relative photoreactivity of the relevant orientational isomers of the precursor complex. However, as judged from the very high photodimerization quantum yield, any reactivity difference between the diastereomeric orientational isomers cannot be very significant as to alter the product distribution.

On the basis of the above discussion, the ratio of the quantum yields of the enantiomers of **2** should be correlated to the thermodynamic parameters for the stability of the precursor complexes in the ground state. A plot of the log of the quantum yield ratio for the enantiomers versus the inverse of temperature is shown in Figure 11. This plot gives the difference in  $\Delta H$  and  $T\Delta S$  for the formation of the 1:2 complexes between the diastereomeric precursor complexes, if one neglects the differences in the molar extinction coefficient and the reactivity of the precursor complexes. The plot gave the estimates of  $-5.8$

**Figure 11.** Plot of log of the quantum yield ratio for the enantiomers of **2** versus the inverse of temperature.

and  $-4.2 \text{ kJ mol}^{-1}$  for  $\Delta\Delta H$  and  $T\Delta\Delta S$  at  $25^\circ\text{C}$ , respectively. This result shows that  $\gamma$ -CDx can discriminate with a moderate difference in affinity an enantiomeric pair of the noncovalent dimers of AC, which produces the enantiomers of the cyclodimer by photodimerization. Thus,  $\gamma$ -CDx provides a chiral template for the enantiodifferentiating photodimerization of AC.

To obtain a higher enantioselectivity, decreasing the temperature was very much effective. Other reaction conditions such as pressure and solvent might also be effective. Another interesting strategy for obtaining a higher selectivity is to chemically modify the  $\gamma$ -CDx. We are now trying to regulate the orientation of AC in the  $\gamma$ -CDx cavity by introducing amino functionalities at the rim of the cavity. This work will be reported in a forthcoming article.

## Conclusions

We have demonstrated that the use of cyclodextrin as a chiral template is an effective and potentially versatile strategy for photochemical supramolecular chirality induction. A relatively high ee of up to 32% was obtained for the isomer of the cyclodimer **2** upon irradiation of AC in aqueous solution at  $25^\circ\text{C}$  in the presence of  $\gamma$ -CDx. The photodimerization was accelerated by the formation of a 1:2 inclusion complex of  $\gamma$ -CDx with AC. The 1:2 inclusion was clearly verified by UV-vis, CD, and  $^1\text{H}$  NMR spectroscopies. Although these spectroscopies provide little information about the structural isomer of the inclusion complex, there should be several structural isomers of the 1:2 inclusion complex which have a different longitudinal orientation of the guest molecules in the cavity. The product isomer distribution primarily depends on the population of these orientational isomers in the ground state before photoreaction, because there is not enough space for the AC molecule to change its orientation within the cavity. Especially, in the lifetime of the excited singlet state, exchanging the orientation is impossible. The enantioselectivity of the photodimerization originates from the difference in the stability of the diastereomeric pair of orientational isomers of the 1:2 inclusion complex in the ground state, which are the precursors of the enantiomers of the cyclodimer **2**. The ee was enhanced by lowering the temperature to 41% at  $0^\circ\text{C}$ . This is the highest value reported for the asymmetric photodimerization in solution.

## Experimental Section

**Materials.** 2-Anthracenecarboxylic acid was purchased from Tokyo Chemical Industry.  $\gamma$ -Cyclodextrin was purchased from Fluka. These were used without any further purification.

**Estimation of the Association Constants.** The association constants were estimated by fitting the observed data for the changes in UV–vis absorption and fluorescence spectra upon titrating the AC solution with  $\gamma$ -CDx to a theoretical model assuming stepwise formation of the 1:2 complex. UV–vis absorption spectra were acquired by the use of a Shimadzu UV-3100 PC spectrophotometer. Fluorescence spectra were obtained using a Hitachi F-4500 spectrofluorometer. The solutions for the titration were made with 25 mM borate buffer (pH 9). For fitting the nonlinear least-squares, a fitting procedure in IGOR Pro was used.

**Photoreaction.** Solutions were made with 25 mM borate buffer (pH 9), sealed in a 1-cm inner diameter Pyrex tube under an Ar atmosphere, immersed in a thermostated liquid medium (aqueous ethylene glycol), and photoirradiated at 366 nm using a medium-pressure mercury lamp equipped with optical glass filters (Toshiba UV-35 and UV-D36C).

**NMR.**  $^1\text{H}$  NMR spectra were acquired using a JEOL JNM-EX 400 spectrometer. Solutions were made with 25 mM borate buffer in  $\text{D}_2\text{O}$  (pD 9).

**HPLC Analysis.** HPLC analyses were performed using a Hitachi system equipped with Inertsil ODS-2 (GL Science), Chiralcel OJ-R, Chiralcel OD-R (Daicel), or tandem columns of Inertsil ODS-2 and Chiralcel OJ-R. For routine analyses, the tandem columns of Inertsil ODS-2 and Chiralcel OJ-R were used. The columns were kept at 35 °C. A mixture of 0.2 M potassium dihydrogen phosphate (adjusted to pH 2.5 with phosphoric acid) and acetonitrile (62:38 by volume for routine analyses) was used as the eluent. The reaction mixture was directly applied to HPLC. The relative yield and % ee were determined by the peak area on the HPLC chromatogram detected by the absorbance at 254 nm.

**Acknowledgment.** The authors thank Ms. Mieko Kunieda-Fukui for assistance in the HPLC analyses, Ms. Yumi Origane for the NMR measurements, and Dr. Guy Hembury for reading and improving the manuscript.

JA016238K